Looking for Synergies in Healthy Upper Limb Motion: A Focus on the Wrist

F. Masiero, I. Fagioli, L. Truppa, A. Mannini, *Member, IEEE*, L. Cappello, *Member, IEEE*, and M. Controzzi, *Member, IEEE*

***Abstract*— Recent studies on human upper limb motion highlighted the benefit of dimensionality reduction techniques to extrapolate informative joint patterns. These techniques can simplify the description of upper limb kinematics in physiological conditions, serving as a baseline for the objective assessment of movement alterations, or to be implemented in a robotic joint. However, the successful description of kinematic data requires a proper alignment of the acquisitions to correctly estimate kinematic patterns and their motion variability. Here, we propose a structured methodology to process and analyze upper limb kinematic data, considering time warping and task segmentation to register task execution on a common normalized completion time axis. Functional principal component analysis (fPCA) was used to extract patterns of motion of the wrist joint from the data collected by healthy participants performing activities of daily living. Our results suggest that wrist trajectories can be described as a linear combination of few functional principal components (fPCs). In fact, three fPCs explained more than 85% of the variance of any task. Wrist trajectories in the reaching phase of movement were highly correlated among participants and significantly more than trajectories in the manipulation phase ($p<0.01$). These findings may be useful in simplifying the control and design of robotic wrists, and could aid the development of therapies for the early detection of pathological conditions.**

***Index Terms*— Upper limb kinematics, functional data analysis, factorial analysis, neurorehabilitation, motor disorders, wrist, postural synergies.**

I. Introduction

UPPER limb mobility is essential in the execution of activities of daily living (ADLs), and its impairment or loss can reduce an individual's quality of life and independence [1], [2]. Modeling healthy upper limb movement is important in neurorehabilitation research, as it gives the opportunity to develop diagnostic tools and therapies to preserve and restore functional abilities in impaired individuals [3], [4]. For example, studies of upper limb motion in healthy individuals can aid the development of (*i*) rehabilitation protocols [4], [5], [6], (*ii*) objective metrics for clinical evaluation [7], [8], [9], and (*iii*) design rules and control strategies for assistive devices, such as prostheses [10], [11], [12] and exoskeletons [13], [14].

While kinematic analysis in lower limb mobility (i.e., gait analysis) is an established tool for clinical evaluation [15], [16], the analysis of upper extremity kinematics for clinical purposes is still an open challenge [17]. There are three main disadvantages in performing motion analysis for the upper limb. First, there is no single most relevant functional activity (akin ground-level walking for lower extremities) [18]. In this regard, while part of the literature focused on selecting relevant ADL tasks [19], [20], other studies aimed at proposing functional tasks for clinical assessments [21], [22] or at identifying task primitives [23]. The wide variety of possible functional tasks hinders from standardizing a motion analysis protocol. Second, upper limb functional activities show a large execution variability (as opposed to the stereotypical gait pattern for lower extremities) [24]. Such variability is primarily due to less stringent constraints for task accomplishment and the redundant number of degrees of freedom of the upper limb's kinematic chain [25]. Finally, the lack of standardized objective metrics obtained via kinematic analysis restrains from communicating relevant clinimetric outcomes, thus deserving further investigations [17], [26].

Past research addressed upper limb motion modeling from a kinematic point of view, by focusing on ranges of motion (RoMs) [27], [28], [29], joint kinematics [30], [31], or kinematic metrics to compare impaired and healthy individuals [32], [33]. Upper limb motion has been addressed also from the neuromuscular point of view, for example by defining models based on muscular synergies extracted from electromyographic activity [34], [35]. None of these works studied the temporal features of human upper limb motion, i.e., the actual shape of the joint trajectories during the task execution. Analyzing the profile of a joint trajectory could allow to spot important details such as the number and temporal location of the angular peaks [36]. This information is lost if the whole trajectory is used to retrieve numbers resuming its behavior (e.g., its RoM or mean value). By contrast, the temporal trend of human joint movements still allows for the extraction of summary metrics, keeping additional objective information that could describe the behavior of a sample population.

Recent studies investigated human upper limb motion from a kinematic viewpoint by leveraging data dimensionality reduction techniques. These techniques can simplify the description of upper limb kinematics in physiological conditions, serving as a baseline to evaluate possible discrepancies

Manuscript received 23 August 2022; revised 26 December 2022; accepted 1 February 2023. Date of publication 9 February 2023; date of current version 14 February 2023. This work was supported by the European Commission under the Horizon 2020 Framework Program for Research and Innovation under Grant B-CRATOS no. 965044. *(F. Masiero and I. Fagioli contributed equally to this work.) (Corresponding authors: F. Masiero; M. Controzzi.)*

This work involved human subjects or animals in its research. Approval of all ethical and experimental procedures and protocols was granted by the Ethics Committee of the Scuola Superiore Sant'Anna under Approval No. 2/2017, and performed in line with the Declaration of Helsinki.

F. Masiero, I. Fagioli, L. Truppa, L. Cappello, and M. Controzzi are with the Department of Excellence and AI, The BioRobotics Institute, Scuola Superiore Sant'Anna, 56127 Pisa, Italy (e-mail: federico.masiero@santannapisa.it; marco.controzzi@santannapisa.it).

A. Mannini is with the IRCCS Fondazione Don Carlo Gnocchi ONLUS, 50143 Firenze, Italy.

Digital Object Identifier 10.1109/TNSRE.2023.3243785

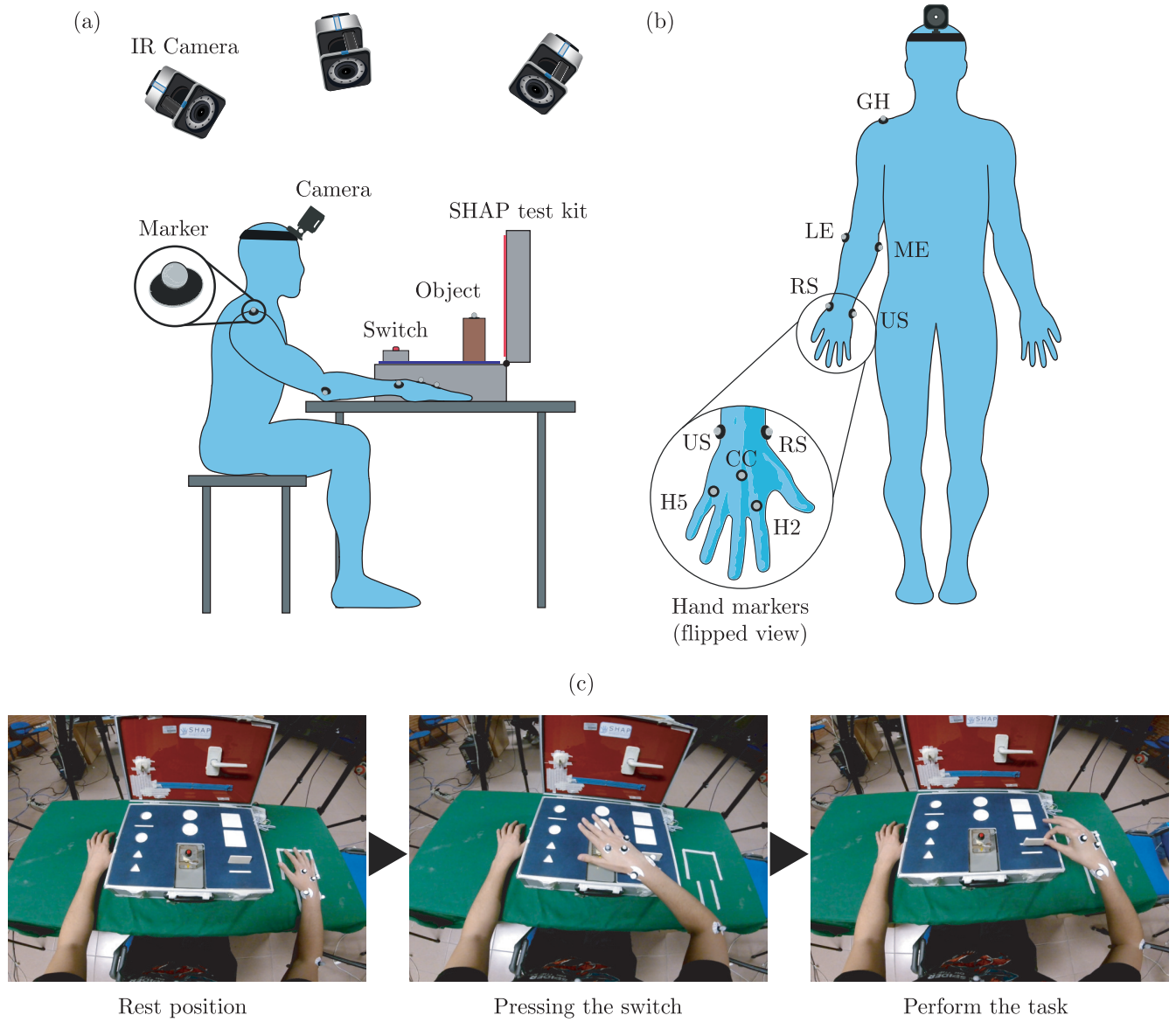

Fig. 1. (a) Experimental setup of the SHAP and the stereophotogrammetric system used for the kinematics recording. From a sitting position, participants performed 14 tasks (Table I). Starting from a rest position (hand palm facing the table), the participant (1) pressed the switch, (2) completed the task, (3) pressed the switch again, and (4) moved back to the rest position. (b) Calibration pose (i.e., n-pose) and marker placement on the right arm of the participant. (c) Summary of a sample task execution (task #5) shown through video frames taken from the head camera.

induced by a pathology [37], or be implemented in a robotic assistive device [38], [39]. For instance, Averta and colleagues used functional principal component analysis (fPCA) [40] and repeated principal component analysis (R-PCA) [41], for investigating dominant modes of variation of functional data in time. Instead, Gloumakov and colleagues [42] adopted an agglomerative clustering technique, grouping tasks in motion categories based on similarity measures between motions. Those approaches allowed to extract temporal features, which cannot be otherwise observed with other data analysis techniques (e.g., principal component analysis), that are only able to capture the static features of a movement [43]. These studies compared task executions without showing evidence of a segmentation process during the data analysis. Although they normalized the time axis of the individual subject, they were not able to bring and compare kinematic data in a common completion time axis. Without the correct temporal alignment, the information extracted from data may be altered, introducing artifacts in the estimate of kinematic patterns and in the quantification of motion variability [44], [45]. Moreover, these studies were limited in presenting primitives extracted from the whole dataset, without any further analysis based on task features such as grasp type and task goal.

The aims of our study are to: (*i*) provide a structured data analysis framework to analyze upper limb kinematic data, and (*ii*) investigate the natural kinematic patterns of the wrist during activities of daily living in healthy participants. To achieve these goals, we recorded the upper limb movements of healthy participants, extracting joint trajectories and segmenting them in reaching and manipulation trends. After segmentation, data were temporally aligned, enforcing temporal alignment also in the retrieved sub-phases (reaching and manipulation), and analysed using fPCA and correlation analysis.

Our method was applied to the wrist focusing on retrieving kinematic patterns in groups of tasks characterized by same grasp type (cylindrical, precision, lateral) or task goal

TABLE I
LIST OF TASKS

ID	Description
	SELF-CONTACT TASKS
1	Touch controlateral armpit
2	Touch chest
3	Touch controlateral temple
4	Touch controlateral hip
	ABSTRACT TASKS
5	Replace triangle
6	Replace plate
7	Replace ball
8	Replace cylinder
9	Replace cup
	INTERACTION TASKS
10	Turn key
11	Turn door handle
12	Open and close zip
13	Page Turning
14	Drinking from glass

Executed tasks, grouped in three categories. Self-contact tasks do not involve the use of objects, whereas abstract and interaction tasks are adapted from the SHAP and they involve the use of objects.

TABLE II
BONY LANDMARKS

Symbol	Description
H2	MCP joint of index finger
H5	MCP joint of little finger
LE	Lateral Epycondyle
ME	Medial Epycondyle
US	Ulnar styloid
RS	Radial styloid
CC	Middle point between RS and US
GH	Glenohumeral rotation center

List of the bony landmarks (markers) used to construct local anatomical frame coordinate systems.

TABLE III
BODY FRAMES DEFINITION

Hand Frame	Forearm Frame	Upper arm Frame
$\mathbf{O_H = CC}$	$\mathbf{O_F = US}$	$\mathbf{O_U = GH}$
$\mathbf{y_H} = \frac{\mathbf{H5 + H2}}{2} - \mathbf{O_H}$ $\mathbf{y_H} = \frac{\mathbf{y_H}}{\|\mathbf{y_H}\|}$	$\mathbf{y_F} = \frac{\mathbf{LE + ME}}{2} - \mathbf{O_F}$ $\mathbf{y_F} = \frac{\mathbf{y_F}}{\|\mathbf{y_F}\|}$	$\mathbf{y_U} = \mathbf{O_U} - \frac{\mathbf{LE + ME}}{2}$ $\mathbf{y_U} = \frac{\mathbf{y_U}}{\|\mathbf{y_U}\|}$
$\mathbf{v} = \mathbf{H2} - \mathbf{O_H}$ $\hat{\mathbf{v}} = \frac{\mathbf{v}}{\|\mathbf{v}\|}$	$\mathbf{v} = \mathbf{US} - \mathbf{RS}$ $\hat{\mathbf{v}} = \frac{\mathbf{v}}{\|\mathbf{v}\|}$	$\mathbf{v} = \frac{\mathbf{LE+ME}}{2} - \mathbf{US}$ $\hat{\mathbf{v}} = \frac{\mathbf{v}}{\|\mathbf{v}\|}$
$\mathbf{x_H} = \frac{\mathbf{y_H} \times \hat{\mathbf{v}}}{\|\mathbf{y_H} \times \hat{\mathbf{v}}\|}$	$\mathbf{x_F} = \frac{\hat{\mathbf{v}} \times \mathbf{y_F}}{\|\mathbf{y_F} \times \hat{\mathbf{v}}\|}$	$\mathbf{z_U} = \frac{\hat{\mathbf{v}} \times \mathbf{y_U}}{\|\mathbf{y_U} \times \hat{\mathbf{v}}\|}$
$\mathbf{z_H} = \mathbf{x_H} \times \mathbf{y_H}$	$\mathbf{z_F} = \mathbf{x_F} \times \mathbf{y_F}$	$\mathbf{x_U} = \mathbf{y_U} \times \mathbf{z_U}$

Reference frame definition for each body segment. Upper arm frame construction is taken from [52]. Hand and forearm frames are custom. Marker names are reported in Table II, and v is an auxiliary vector.

(self-touching, involving object manipulation). With the correlation analysis we aimed to assess inter-subject variability when performing the same task or when performing different tasks belonging to the same category (i.e., with the same grasp type or task goal).

The proposed data analysis framework can be used to compactly describe joint trajectories as a combination of functional principal components. Extracting this information from many participants allows to trace a baseline behavior to compare individuals from different populations (e.g., with a different pathology). The analysis of the wrist also proved that most of the correlation was concentrated in the reaching phase, suggesting that its patterns could be good kinematic indicators for healthy individuals and providing repeatable patterns associated to grasp type (e.g., cylindrical) and task goal (e.g., self-touching tasks).

Our results may also be relevant for the prosthetic field, consolidating the importance of designing wrist rotators (implementing PS), but also highlighting the importance of FE for the completion of self-touching tasks. In this view, this work provides reference wrist trajectories that can be considered either in the mechanical design of underactuated robotic wrists or for the control of a multi-articulated robotic wrist based on postural synergies.

II. MATERIALS AND METHODS

A. Experiments

Thirteen unimpaired right-handed volunteers (age range: 22 – 30 years, 9 males and 4 females) with no diagnosed motor disorders were enrolled in this study. The study was performed in accordance with the Declaration of Helsinki and approved by the Ethics Committee of the Scuola Superiore Sant'Anna (approval number 2/2017). All participants gave written informed consent before participating in the study. Participants were sit at a table and were instructed to repeatedly complete a trial consisting of the execution of a set of 14 tasks, provided in a random order (Fig.1a,c) and representative of the ADLs (Table I). In the instructions, the experimenter emphasized that the whole movement should be performed in a natural fashion. The tasks were selected based on a set of movements driven by the studies of grasping taxonomies [46], [47], and upper limb workspace analysis [48], [49]. These were subdivided into self-contact tasks (#1-4), abstract tasks (#5-9), and interaction tasks (#10-14), adapted from [50] and [51]. In particular, tasks from 5 to 14 were selected or adapted from a standard functional test, i.e., the SHAP [5]. Participants were asked to repeat each task ten times, and each repetition, or trial, consisted in the following sequence of actions: from a fixed starting position with the palm facing the table, the participant pressed a switch, performed the task, pressed again the switch, and moved back to the starting position.

Upper limb movements were tracked with a system based on optical reflective markers attached to the upper limb body segments. To position the markers, we followed the ISB guidelines for the whole upper limb kinematic chain [52], except for the hand/wrist system, for which we used a custom configuration inspired by the work of Murgia et al. [53] (Fig.1b). Before the experimental sessions, each participant was asked to keep a static n-pose to calibrate the participant-specific

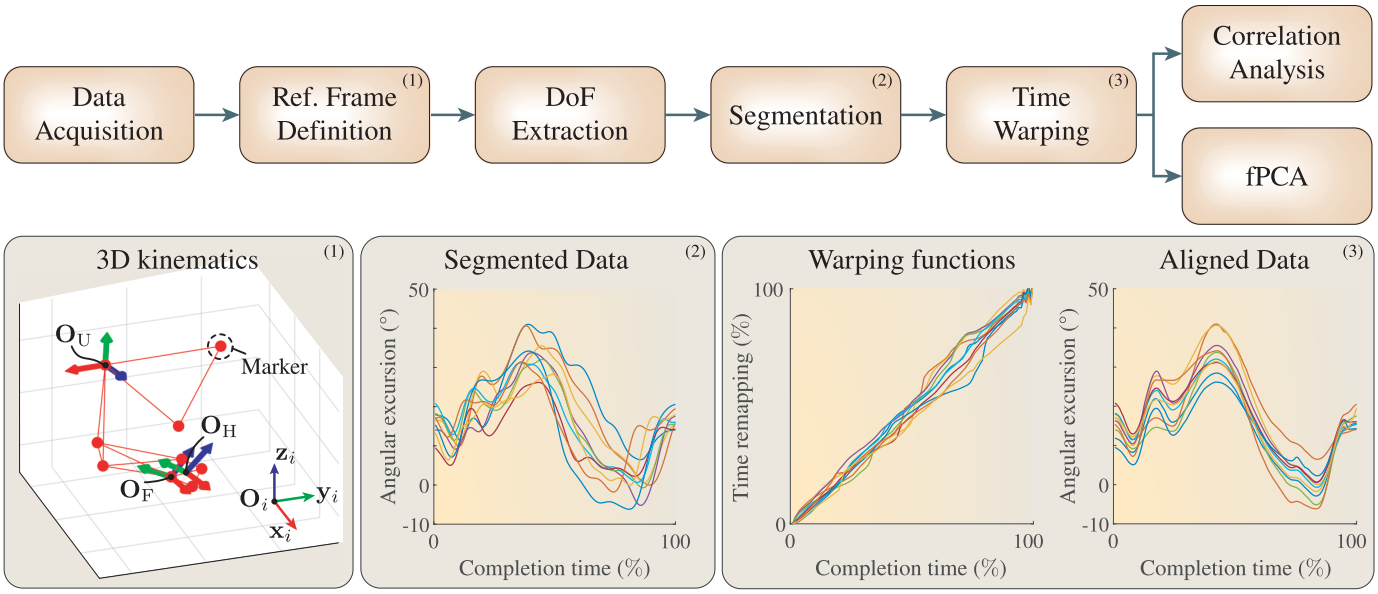

Fig. 2. Diagram of the data processing and analysis framework. After the acquisition of kinematics data (e.g., through a stereophotogrammetric system), a reference frame for each body segment is defined. By computing the relative orientation among adjacent segments, the temporal trends of the joint DoFs are extracted. These are segmented to retrieve only the informative regions of the task executions. Finally, before data analysis, the execution of each trial is temporally aligned through a warping procedure to highlight relevant features among multiple repetitions.

TABLE IV
EXPLAINED VARIANCE IN ALL TASKS AND TASKS WITHOUT AN OBJECT

		FE	RUD	PS
All tasks	fPC1	73	63	67
	fPC2	82	78	86
	fPC3	90	86	93
No Objects	fPC1	69	75	86
	fPC2	84	83	94
	fPC3	93	91	98

Explained variance retrieved by applying fPCA to all the tasks together (top) or tasks without an object (down). Values are reported for each DoF (FE, RUD, and PS) and increasing number of fPCs (up to three).

TABLE V
EXPLAINED VARIANCE IN GRASPING TASKS

		FE		RUD		PS	
		R	**M**	**R**	**M**	**R**	**M**
Power	fPC1	83	59	87	80	84	88
	fPC2	94	88	97	93	98	97
	fPC3	98	94	99	97	99	99
Precision	fPC1	82	46	93	48	90	45
	fPC2	94	70	98	82	98	70
	fPC3	98	85	99	90	99	91
Lateral	fPC1	68	80	84	65	88	59
	fPC2	90	97	93	90	98	86
	fPC3	96	99	98	95	99	94

Explained variance retrieved by applying fPCA on grasping tasks (#5-14), which are grouped based on the grasp type [46]. Values are reported for each DoF (FE, RUD, and PS) and increasing number of fPCs (up to three), both for reaching (**R**) and manipulation phase (**M**).

marker positions (Fig.1b). Participants were asked to wear an action camera on their forehead, recording at 60 fps the task execution from their perspective. These recordings were used to group the tasks by fitting the observed grasps into three categories: power grasp, lateral grasp, and precision (pinch) grasp. Reflective markers were also placed on the objects used during the experiment in order to segment reaching and manipulation phases. We used 6.4 mm Reflective Pearl Markers to track the hand of the participants, and 9.5 mm Reflective Pearl Markers to track the remaining upper limb chain and the objects. The markers' position in space was recorded with a sampling frequency of 100 Hz through an eight-camera stereophotogrammetric system (Vicon MX3, Oxford, U.K.). The system was calibrated before each experimental session to achieve submillimetric resolution in the target workspace.

B. Data Analysis

Markers' positions were imported in MATLAB R2019b (Natick, Massachusetts, USA) and used to reconstruct the kinematics of the upper limb body segments. Using the marker definitions reported in Table II, we built three reference systems in the hand, forearm, and upper arm, according to the expressions presented in Table III. Then, we extracted the time series of the wrist degrees of freedom (DoFs) from the rotation matrices describing the relative orientation between adjacent body segments. In particular, the extracted DoFs were flexion/extension (FE), pronation/supination (PS), and radial/ulnar deviation (RUD). FE and RUD were extracted from the relative orientation between the hand and forearm, and PS was extracted from the relative orientation between the forearm and the upper arm.

Each task was segmented in trials using a switch signal acquired through a NI DAQ USB-6009 connected to a computer running LabVIEW 2017 and synchronized to the stereophotogrammetric system. The ten repetitions of each task were temporally aligned using a time-warping procedure, i.e., the elastic regression algorithm proposed by Tucker et al. [45] (see Appendix I). This allowed to achieve temporal alignment of salient events of the tasks, independently of their execution times. To align all three DoFs of the wrist in a trial, the

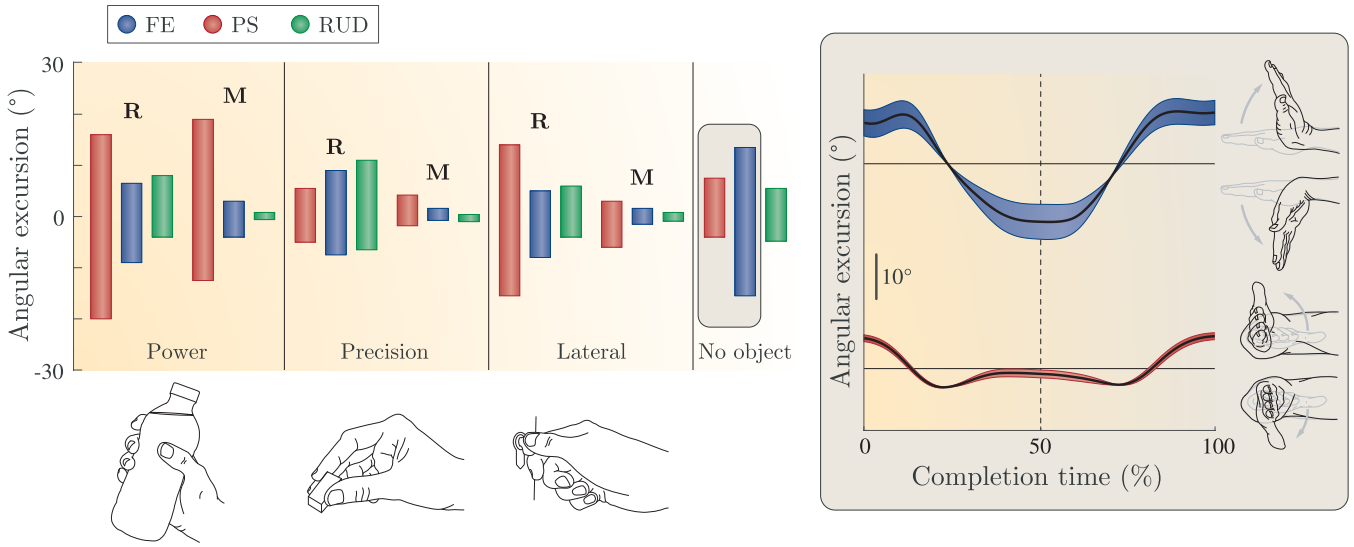

Fig. 3. (Left) Average angular excursion of FE (blue), PS (red), and RUD (green) for self-contact tasks (no object) and tasks with the same grasp type (power, precision, lateral), divided in reaching (R) and manipulation (M). (Right) A detailed view of the mean curve (black) and first fPC (blue and red shapes) for FE and PS in self-contact tasks.

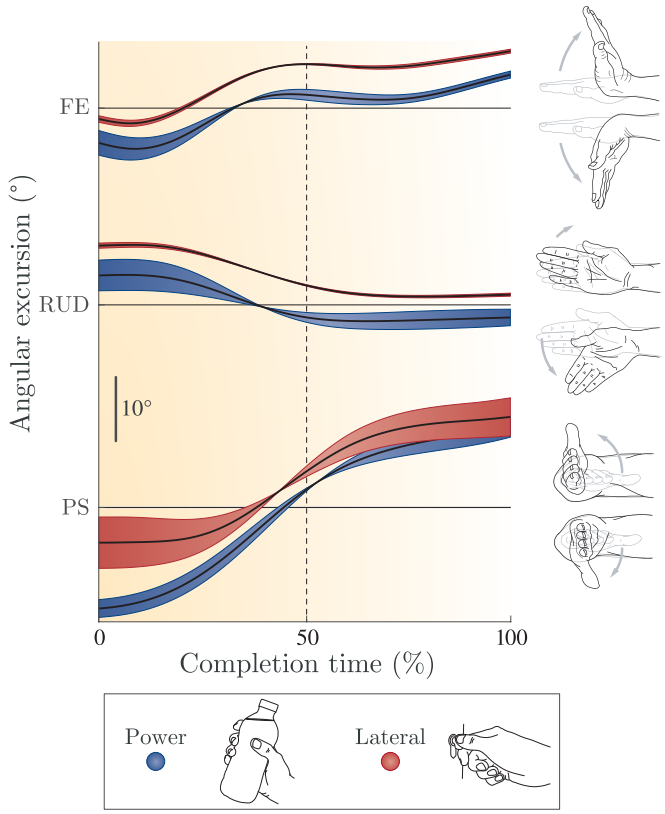

Fig. 4. Average reaching phase temporal trends of the wrist DoFs while performing tasks involving power (blue) or lateral (red) grasps. Similar trends can be observed for both grasp types and for all DoFs.

warping function from the time series of the DoF exhibiting the widest angular span was used to align the two remaining DoFs. For instance, for task #1 (touching the contralateral temple) and participant #1, we used the PS time series to derive the temporal misalignment of the trials (i.e., the warping function, Fig.2). The derived warping functions were then used to align the FE and RUD time series of that specific task (Fig.2). For a certain task, the DoF chosen for the alignment may not be the same for every participant.

Trials involving the use of an object (tasks #5-14) were further segmented into a reaching phase and a manipulation phase using the object's markers position before undergoing to time warping. For instance, abstract tasks (#5-9) were segmented in correspondence to the minimum euclidean distance between the marker on the object and the center of the hand. The temporally aligned curves were then averaged in order to obtain a mean curve for each task performed by a participant. All the obtained curves (both unsegmented and segmented) were finally resampled to achieve a common normalized time axis (as percentage of the task completion) for comparison.

Two analyses were then performed: a functional Principal Components Analysis (fPCA), and a correlation analysis. fPCA is a statistical method used to study the dominant variation modes in temporal series (see Appendix II). To perform this analysis, we used the PACE package [54], implementing the fPCA by conditional expectation. We ran the algorithm on the average curves, considering: (i) all tasks together (as presented in previous studies [40], [41], [42]), (ii) all the self-touching tasks, and the (iii) reaching and (iv) manipulation phases for all the tasks associated to a specific grasp type.

For the correlation analysis, we used the Spearman's rank correlation coefficient, r. This coefficient assesses how well an arbitrary monotonic function can describe a relationship between two variables without making assumptions on their frequency distribution (nonparametric statistic). The correlation coefficient was used to assign a score to the similarity of the analyzed nonlinear time series representing the wrist DoFs trajectories. Accordingly, for the groups (ii), (iii) and (iv), we computed different correlation matrices. We investigated two types of correlations: (1) the correlation of the same task performed by different participants (i.e., i-th and j-th participant), and (2) the correlation between tasks from the same group (i.e., (ii), (iii) and (iv)).

To confirm the outcomes of the correlation analysis, a statistical analysis on the distribution of the correlation coefficients moduli ($|r|$) of reaching and manipulation trajectories was performed. After the verification of the non-normality of the data (i.e., using the Lilliefors test) we conducted a non-parametric one-sided test (i.e., the Wilcoxon rank sum test)

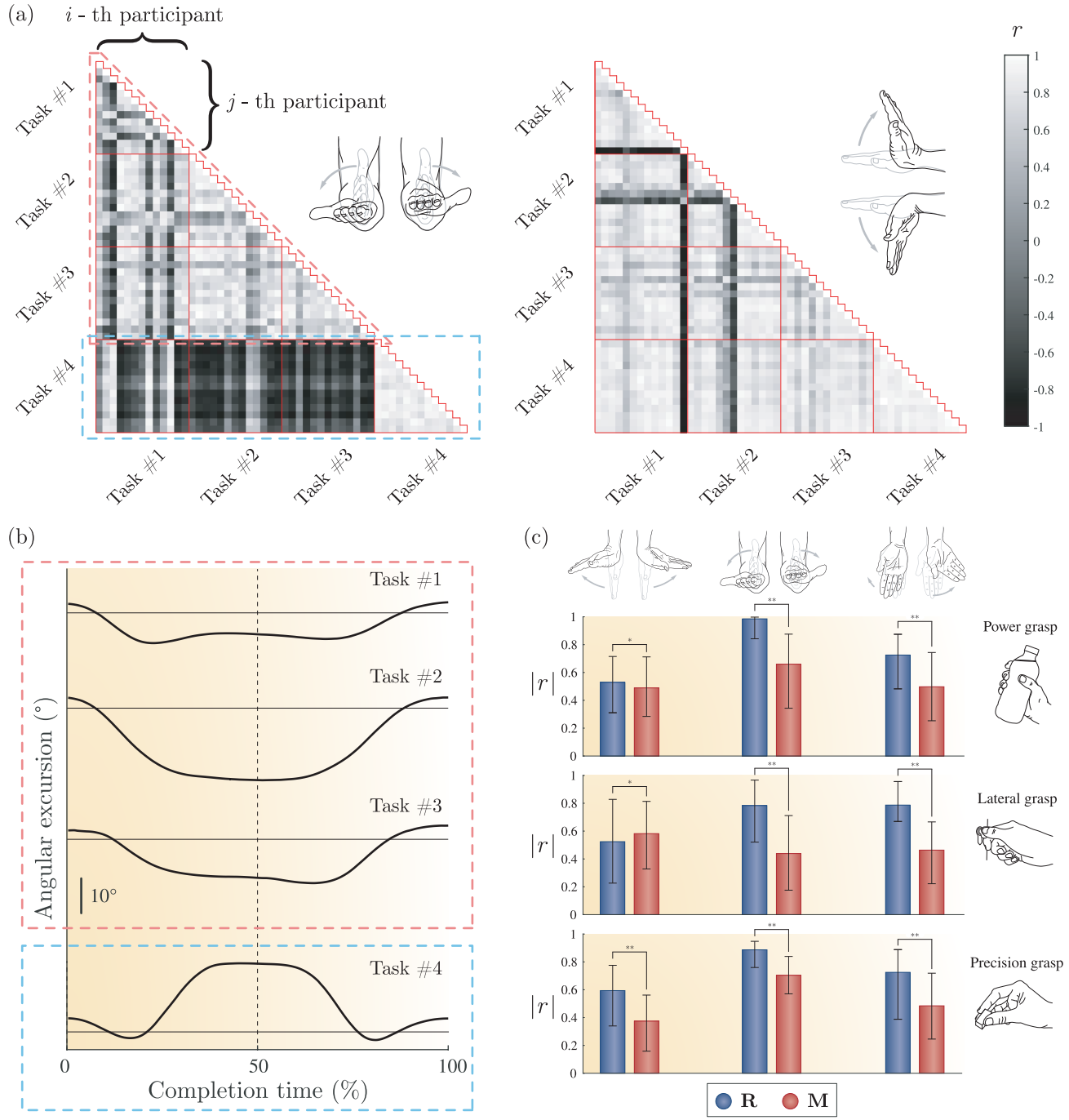

Fig. 5. (a) Correlation among self-touching tasks for the PS (left panel) and FE (right panel) trajectories. Because of their symmetry, only the lower-left half of the correlation matrix is shown. Both correlation matrices show the correlation coefficient, *r*, between the *i*-th and the *j*-th subject. The matrix on the left panel indicates that tasks #1-3 are positively correlated among themselves (clearer colors) whereas they are strongly negatively correlated with task #4 (darker colors) when considering PS. By contrast, the matrix on the right panel shows that all the tasks share a high positive correlation when considering the FE. (b) Temporal trends of the average curves for tasks #1-4, offering visual evidence of the correlation values in the corresponding correlation matrix. (c) Box plots of the correlation coefficients moduli, grouping tasks based on grasp type and DoF. The blue bars are relative to reaching trajectories, the red ones to manipulation trajectories. The statistical significance between pairs of distributions is indicated, based on the outcome of the Wilcoxon rank sum test (i.e., * stands for $p < 0.05$ and ** for $p < 0.01$).

on the two distributions (reaching and manipulation phases) grouping the tasks based on the grasp type and the DoF.

III. Results

The fPCA computed on the whole set of tasks allowed us to infer that the first fPC, by itself, accounts for 73%, 63%, and 67% of the variation with respect to the mean function for FE, RUD, and PS, respectively (Table IV). Considering three fPCs led to an explained variance above 85% for every DoF (Table IV).

In the self-touching tasks (tasks #1-4), the variance explained by the first fPC was 69%, 75%, and 86%, respectively for FE, RUD, and PS (Table IV). The explained variance was more than 80% for two fPCs and more than 90% for three fPCs, with a peak of 98% for PS (Table IV).

In grasping tasks (tasks #5-14), the reaching phase was characterized by values of explained variance larger than the manipulation phase (Table V). The first fPC always accounted for more than 80% of the variance, except for the FE in lateral grasp, for which the explained variance was 68%. The second

and third fPCs always led to more than 90% and 95% of explained variance, respectively.

Angular excursions are summarized in Fig.3 for FE, PS, and RUD for different task groups (i.e., tasks involving a specific grasp type or self-touching tasks). Notably, the reaching phase (R) always involved an angular excursion larger than the manipulation phase (M). This difference was more pronounced in FE and RUD, which had a very limited excursion in precision and lateral grasp. Tasks without an object, being those not segmented in different task phases (reaching and manipulation), exhibited a clear symmetric shape around the 50% of the completion time.

The functional principal components extracted for curves related to the manipulation phase explained lower variance with respect to those extracted for the reaching phase, independently of the grasp type (Table V). For instance, in the case of precision grasp, the explained variance for the manipulation phase accounted by the first fPC was around 40% smaller than the reaching phase, for all DoFs. The use of three fPCs still led to an explained variance larger than 85%. Notably, in the case of power grasp and lateral grasp, the use of only two fPCs allowed to infer more than the 85% of the explained variance.

Similar time trends were observed for all DoFs in the reaching phase of power and lateral grasp (Fig.4). In detail, the RUD followed a monotonic decreasing trend with an inflexion point at around 40% of the completion time. A mirrored shape was observed for the PS, with an inflexion point close to the 50% of task completion. Interestingly, the FE showed the same non-monotonic pattern. The angular ranges involved were also comparable (Fig.3,4).

The results of the correlation analysis unveiled common patterns of movement between tasks. When considering self-contact tasks, FE proved to be highly correlated among participants. Few exceptions were observed, e.g., participant #13 performing task #1 and participants #6 and #7 performing task #2 (Fig.5a, right panel). In general, the PS trend for tasks #1-3 was positively correlated among participants, and negatively correlated with respect to task #4 (Fig.5a, left panel). As shown in (Fig.5b), the trends of the correlated tasks (#1-3) are similar in shape, and they resemble the flipped shape of the negatively correlated task (#4). By comparing the distribution of the modulus of the correlation coefficient ($|r|$, to consider correlation independently on the sign) and grouping tasks based on the grasp type, we found that the reaching trajectories were more correlated than manipulation trajectories (Fig.5c). In fact, median correlation coefficients of reaching trajectories were significantly larger than those computed for manipulation trajectories ($p < 0.01$, Fig.5c). The only exception was FE during lateral grasps, for which we observed the opposite result ($p < 0.05$).

Although the distributions of the absolute values of the correlation coefficients for the RUD trajectories were comparable to the ones involving the PS, no relevant pattern was observed. More in general, we did not find any kinematic pattern in the manipulation curves (for any DoF).

IV. Discussions and Conclusion

The aims of this study were to (*i*) provide a structured methodology for the analysis of upper limb motion, and to (*ii*) employ it to analyze wrist patterns in healthy participants performing tasks of daily living. We decided to apply the proposed methodology solely to the kinematics of the wrist, although the same methodology could be applied to other joints. Our interest for the wrist was motivated by its importance in the completion of the ADLs [55], whose study and substitution was largely overlooked in past research in the prosthetic field [56], [57]. Gaining useful insights on the wrist behavior in relation to grasp types and task goals could help in the design of novel robotic wrists, mimicking the kinematics of their natural counterpart while keeping a compact design (as imposed in the prosthetic field application). Instead, from the neurorehabilitation perspective, finding kinematic descriptors of upper limb kinematics in physiological conditions provides a baseline to evaluate possible discrepancies induced by a pathology [41]. Our methodology can promote the extraction of kinematic objective metrics from upper limb motion data exploiting a data dimensionality reduction technique, i.e. fPCA. Our analysis framework is compatible and (to some extent) complementary to metrics proposed in other kinematic studies [17], [36], meaning that its use does not prevent the extraction of standard descriptors (e.g., RoM, jerk, average velocity). Other investigators recently proved that the combination of these methodologies could contribute to the inference of motor disabilities [37]. The novelty of the proposed work resides not only in the adopted methodology, but also in the extended correlation analysis performed between the extracted DoFs grouped by grasp type and task goal.

We built our dataset exploiting the SHAP test, which is a clinically validated hand function test for the assessment of musculoskeletal and neurological conditions [5]. Data were recorded with a stereophotogrammetric system, which is known to be a reference standard for its high resolution and accuracy [58]. Nonetheless, the proposed data analysis methodology is compatible with other motion tracking technologies (e.g., IMUs, cameras) [59], [60].

After the extraction of the wrist DoFs, we temporally aligned the executions of the tasks for all subjects. The successful implementation of temporal alignment required many repetitions, motivating us to record 10 times the execution of each task. Differently from previous studies [40], [41], [42], we also exploited task segmentation to enforce the temporal alignment for the whole dataset in a unique common normalized time axis. This is crucial, since the lack of temporal alignment (also between different tasks), can lead to unfair comparisons, resulting in the wrong estimation of kinematic patterns and their variability. We then analyzed the preprocessed data using fPCA and correlation analysis. We analyzed the executed tasks both dividing them by grasp type (i.e., power, precision, and lateral), considering task goal (i.e., self-touching tasks and tasks involving objects manipulation), and by separately considering each phase (i.e., reaching and manipulation).

Functional PCA summarizes kinematic trajectories as a linear combination of few principal components (Fig.2). In tasks that required handling an object, we found that PS was the predominant DoF, both in the reaching and manipulation phase (Fig.3). In fact, PS showed the highest angular range (also in relative terms, i.e., with respect to the overall joint RoM), and its trend could be explained by fewer fPCs. This justifies the tendency in upper limb prosthetics in developing powered wrist joints that only implement PS. In self-contact tasks, FE was the DoF exhibiting the highest angular excursions (Fig.3). In those tasks, FE and PS patterns of movement were highly correlated among different participants (Fig.5a).

Interestingly, a strong negative correlation was observed for the PS between task #4 and tasks #1-3. This may be due to the different location of the target body part (inferior part of the body or superior part of the body). In addition, the use of a single fPC could effectively summarize the PS trend (Table IV). From the neurorehabilitation perspective, these results suggest that wrist rehabilitation protocols should mostly target FE and PS. Unexpectedly, RUD was uninformative, exhibiting a very small angular excursion and no relevant kinematic pattern (except in the reaching phase of self-touching tasks, Fig.4). This outcome may be due to the selected set of tasks; however, independently on this outcome, having its trend at disposal could still serve as a baseline for comparing the same tasks performed by impaired individuals. Future studies with additional data may help discern the role of this DoF in ADLs.

Our results confirmed that the wrist movements in daily living activities could be effectively summarized using fPCA, i.e., more than 85% of the explained variance could be explained using only three fPCs. These findings would not have been so relevant if the temporal alignment was not considered as a data preprocessing step. Even if temporal alignment has been used in previous works [40], [42], our study introduces a further time alignment step thanks to task segmentation. In fact, part of the novelty of this work was the direct analysis of distinct phases of task completion. We analyzed the execution of tasks involving an object considering reaching and manipulation phases, separately. This allowed us to infer that univocal patterns of movement of the wrist were concentrated during the reaching phase of tasks that require the same kind of grasp, while it was more difficult to observe patterns of movement in the manipulation phase. In fact, the reaching curves showed to (*i*) be more correlated (Fig.5c) and (*ii*) have less inter-participant variability (Table V) with respect to the manipulation curves. These results demonstrate that factors typically influencing task completion (e.g., object positioning, object contact location, and anthropometric differences) did not significantly affect the variability of the reaching phase in the workspace range of the SHAP (around 1 m^3). Since the goal of the manipulation phase is to achieve a target pose of the manipulated object, it is reasonable to observe a larger variability in this phase. This is inherited by the redundancy of the human upper limb kinematic chain, capable of producing different spatial and temporal trajectories associated to the same final goal (e.g., depending on the grasp location achieved during reaching).

The obtained outcomes suggest that wrist reaching patterns are good kinematic indicators for healthy participants and may be used as references to diagnose neurological pathologies. Furthermore, our results highlighted the importance of task segmentation (in reaching and manipulation phases), which allowed to understand where most of the task repeatability was located.

Our experiment targeted only tasks involving the dominant hand. Bimanual tasks were not taken into consideration because they are known to be more complicated in terms of repeatability and grasp modality. Including bimanual tasks in a biomechanical study may be the starting point of a future work. Our analysis was also limited to a small number of healthy participants, performing a set of tasks starting from a unique workspace location. Future improvements of our investigation will consider extending the available dataset (e.g., including also non-healthy participants), addressing the effect of starting position (which might have affected the observed RoMs), collecting more tasks executions, and analyzing the remaining upper limb joints. For example, using the same experimental setup and applying the presented methodology to the whole upper limb kinematic chain could be a valuable instrument to study compensatory movements in upper limb amputees [55], [57].

To conclude, we proposed a structured methodological framework to study upper limb joint kinematics. The methodology is structured in the sense that it (*i*) can compare different tasks (performed by different subjects) in a common completion time axis (leveraging task segmentation) and (*ii*) allows to extract objective metrics from kinematic data. By applying this framework to the study of the wrist, we showed that it is feasible to extract biomechanical patterns related to grasp type and task goal. While our methodology could be integrated into the data analysis pipeline of a rehabilitation protocol, the patterns obtained could serve as a baseline for describing the kinematics of healthy participants, helping to diagnose motor disorders (by comparing participants kinematics' to the healthy dataset), and aiding the development and control of robotic assistive devices (e.g., by implementing such profiles in the robotic joint motion). Further research should be performed to investigate the use of the proposed framework in clinical settings, and for the prototyping and control of the next generation assistive devices.

Appendix I
Temporal Alignment Using Elastic Regression

The variability exhibited by different observations of the same time-series (e.g., the repetitive execution of a task performed by the same subject) can be expressed in terms of amplitude (y-axis) and phase (x-axis) variability. Many existing techniques for functional data analysis neglect phase variability, implicitly assuming that the observed functions are already temporally aligned. Time-warping refers to the process of aligning data along their time axis, thus reducing phase variability. Phase variability among the original curves is captured by the warping functions.

Here, we summarize a time-warping technique based on elastic regression [45]. Without loss of generality, let q be a continuous real-valued function in the normalized domain [0, 1], and let $\mathcal{Q}$ denote the set of all such functions. Let Γ be the set of warping functions:

$$\Gamma = \left\{ \gamma \,:\, [0,\,1] \to [0,\,1] \;\middle|\; \gamma(0) = 0,\ \gamma(1) = 1 \right\}.$$

The elements of Γ are boundary-preserving, invertible, and differentiable (i.e., diffeomorphisms). For any $q \in \mathcal{Q}$ and $\gamma \in \Gamma$, the composition $q \circ \gamma$ denotes the time-warping of q by γ. In a pairwise alignment problem, the goal is to align any couple of functions q_1 and q_2, in our case representative of different repetitions of the same task. For the present alignment method, there is the need to introduce $f : [0,\,1] \to \mathbb{R}$, the square-root slope function (SRSF) of q:

$$f(t) = \operatorname{sign}\left(\dot{q}(t)\right) \sqrt{|\dot{q}(t)|}.$$

If we warp a function q by γ, the SRSF of $q \circ \gamma$ is $\tilde{f}(t) = f(\gamma(t))\sqrt{\dot{\gamma}(t)}$. Therefore, it can be shown that for any q_1, $q_2 \in \mathcal{Q}$, and $\gamma \in \Gamma$, the isometry property holds:

$$\|f_1 - f_2\| = \|(f_1, \gamma) - (f_2, \gamma)\|,$$

where f_1, f_2 are SRSFs of q_1, q_2, respectively. This property suggests a distance between functions that is invariant to their warpings:

$$D_y(q_1, q_2) = \inf_{\gamma \in \Gamma} \|f_1 - (f_2, \gamma)\|.$$

Therefore, we can align the SRSFs of any two functions and then map them back to $\mathcal{Q}$ to obtain the aligned functions.

The idea behind temporal alignment is to time-warp data with respect to a representative time-series. From the aligned SRSFs, it is possible to compute each aligned functions as:

$$\tilde{q}_i(t) = q_i(0) + \int_0^t \tilde{f}_i(s)|\tilde{f}_i(s)|\,\mathrm{d}s.$$

The aligned data can then be processed with traditional functional data analysis techniques, e.g., fPCA.

Appendix II
Functional Principal Component Analysis

Functional principal component analysis (fPCA) is used to discover dominant modes of variation in functional data [44]. This data analysis technique is able to capture relevant patterns if data are temporally aligned (see Appendix I). Here, we summarize the basic theory of fPCA applied to upper limb kinematics.

Let us assume a kinematic chain with l DoFs, in which the j-th joint angle q_j is described by a time-series with N available observations, and $j = 1, \ldots, l$. Let us also assume that each time-series is defined over a common normalized time axis $t \in [0,\ 1]$. A generic signal representing the temporal profile of a joint can be decomposed as a weighted sum of basis elements $\xi_j^i(t)$, or fPCs:

$$q_j(t) \approx \bar{q}_j(t) + \sum_{i=1}^{s_{max}} \alpha_j^i \cdot \xi_j^i(t)$$

where α_j^i are weights (or scores), s_{max} is the number of basis elements considered and $\bar{q}$ is the average of $q(t)$ across the N observations. The output of the fPCA, which is computed independently for each joint, is a basis of functions $\{\xi_j^1, \ldots, \xi_j^{s_{max}}\}$ that maximizes the explained variance of upper limb motions collected in the dataset. The first fPC $\xi_j^1(t)$ is the function that solves the following optimization problem:

$$\max_{\xi_j^1} \sum_{k=1}^{N} \left(\int_0^1 \xi_j^1(t) \cdot q_j^k(t)\,\mathrm{d}t \right)^2$$

$$\text{such that} \quad \|\xi_j^1(t)\| = \int_0^1 \left(\xi_j^1(t)\right)^2 \mathrm{d}t = 1$$

Subsequent fPCs $\xi_j^s(t)$ are the functions that solve the above optimization problem, with the additional constraint of orthogonality, i.e.,

$$\int_0^1 \xi_j^s(t)\xi_j^k(t)\,\mathrm{d}t = 0, \quad \forall k \in \{1, \ldots, p-1\}$$

where p refers to the number of the already computed fPCs. The interested reader can find additional details in [44].

Acknowledgment

The authors thank Dr. Michelangelo Guaitolini, for his assistance.

References

[1] D. Nowak, "The impact of stroke on the performance of grasping: Usefulness of kinetic and kinematic motion analysis," *Neurosci. Biobehav. Rev.*, vol. 32, no. 8, pp. 1439–1450, Oct. 2008.
[2] H. Shahsavari et al., "Upper limb amputation; care needs for reintegration to life: An integrative review," *Int. J. Orthopaedic Trauma Nursing*, vol. 38, Aug. 2020, Art. no. 100773.
[3] M. A. Murphy and C. K. Häger, "Kinematic analysis of the upper extremity after stroke–how far have we reached and what have we grasped?" *Phys. Therapy Rev.*, vol. 20, no. 3, pp. 137–155, 2015.
[4] A. M. Valevicius et al., "Characterization of normative hand movements during two functional upper limb tasks," *PLoS ONE*, vol. 13, no. 6, Jun. 2018, Art. no. e0199549.
[5] P. J. Kyberd et al., "Case studies to demonstrate the range of applications of the southampton hand assessment procedure," *Brit. J. Occupat. Therapy*, vol. 72, no. 5, pp. 212–218, May 2009.
[6] F. Clemente, M. D'Alonzo, M. Controzzi, B. B. Edin, and C. Cipriani, "Non-invasive, temporally discrete feedback of object contact and release improves grasp control of closed-loop myoelectric transradial prostheses," *IEEE Trans. Neural Syst. Rehabil. Eng.*, vol. 24, no. 12, pp. 1314–1322, Dec. 2015.
[7] B. Rohrer et al., "Movement smoothness changes during stroke recovery," *J. Neurosci.*, vol. 22, no. 18, pp. 8297–8304, Sep. 2002.
[8] M. A. Murphy, C. Willén, and K. S. Sunnerhagen, "Kinematic variables quantifying upper-extremity performance after stroke during reaching and drinking from a glass," *Neurorehabil. Neural Repair*, vol. 25, no. 1, pp. 71–80, 2011.
[9] M. Blaszczyszyn, A. Szczesna, J. Opara, M. Konieczny, P. Pakosz, and S. Balko, "Functional differences in upper limb movement after early and chronic stroke based on kinematic motion indicators," *Biomed. Papers*, vol. 162, no. 4, pp. 294–303, Nov. 2018.
[10] M. Controzzi, F. Clemente, D. Barone, A. Ghionzoli, and C. Cipriani, "The SSSA-myhand: A dexterous lightweight myoelectric hand prosthesis," *IEEE Trans. Neural Syst. Rehabil. Eng.*, vol. 25, no. 5, pp. 459–468, May 2017.
[11] L. Resnik, S. L. Klinger, and K. Etter, "The DEKA arm: Its features, functionality, and evolution during the veterans affairs study to optimize the DEKA arm," *Prosthetics Orthotics Int.*, vol. 38, no. 6, pp. 492–504, 2014.
[12] M. Laffranchi et al., "The hannes hand prosthesis replicates the key biological properties of the human hand," *Sci. Robot.*, vol. 5, no. 46, Sep. 2020, Art. no. eabb0467.
[13] T. Nef, M. Guidali, and R. Riener, "ARMin III—Arm therapy exoskeleton with an ergonomic shoulder actuation," *Appl. Bionics Biomech.*, vol. 6, no. 2, pp. 127–142, Jul. 2009.
[14] E. Trigili et al., "Design and experimental characterization of a shoulder-elbow exoskeleton with compliant joints for post-stroke rehabilitation," *IEEE/ASME Trans. Mechatronics*, vol. 24, no. 4, pp. 1485–1496, Aug. 2019.
[15] D. A. Winter, "Kinematic and kinetic patterns in human gait: Variability and compensating effects," *Hum. Movement Sci.*, vol. 3, nos. 1–2, pp. 51–76, Mar. 1984.
[16] D. Ricardo, J. Teles, M. R. Raposo, A. P. Veloso, and F. João, "Test-retest reliability of a 6DoF marker set for gait analysis in cerebral palsy children," *Appl. Sci.*, vol. 11, no. 14, p. 6515, Jul. 2021.
[17] A. Schwarz, C. M. Kanzler, O. Lambercy, A. R. Luft, and J. M. Veerbeek, "Systematic review on kinematic assessments of upper limb movements after stroke," *Stroke*, vol. 50, no. 3, pp. 718–727, Mar. 2019.
[18] A. Kontaxis, A. G. Cutti, G. R. Johnson, and H. E. J. Veeger, "A framework for the definition of standardized protocols for measuring upper-extremity kinematics," *Clin. Biomech.*, vol. 24, no. 3, pp. 246–253, Mar. 2009.
[19] D. J. Magermans, E. K. J. Chadwick, H. E. J. Veeger, and F. C. T. van der Helm, "Requirements for upper extremity motions during activities of daily living," *Clin. Biomech.*, vol. 20, no. 6, pp. 591–599, Jul. 2005.
[20] A. S. Cornwell, J. Y. Liao, A. M. Bryden, and R. F. Kirsch, "Standard task set for evaluating rehabilitation interventions for individuals with arm paralysis," *J. Rehabil. Res. Develop.*, vol. 49, no. 3, p. 395, 2012.
[21] K. Petuskey, A. Bagley, E. Abdala, M. A. James, and G. Rab, "Upper extremity kinematics during functional activities: Three-dimensional studies in a normal pediatric population," *Gait Posture*, vol. 25, no. 4, pp. 573–579, Apr. 2007.
[22] M. Longhi, A. Merlo, P. Prati, M. Giacobbi, and D. Mazzoli, "Instrumental indices for upper limb function assessment in stroke patients: A validation study," *J. NeuroEng. Rehabil.*, vol. 13, no. 1, pp. 1–11, Dec. 2016.

[23] H. M. Schambra, A. Parnandi, N. G. Pandit, J. Uddin, A. Wirtanen, and D. M. Nilsen, "A taxonomy of functional upper extremity motion," *Frontiers Neurol.*, vol. 10, p. 857, Aug. 2019.
[24] C. J. van Andel, N. Wolterbeek, C. A. Doorenbosch, D. H. Veeger, and J. Harlaar, "Complete 3D kinematics of upper extremity functional tasks," *Gait Posture*, vol. 27, no. 1, pp. 120–127, Jan. 2008.
[25] K. Davids, S. Bennett, and K. M. Newell, *Movement System Variability*. Champaign, IL, USA: Human Kinetics, 2006.
[26] A. D. L. Reyes-Guzmán, I. Dimbwadyo-Terrer, F. Trincado-Alonso, F. Monasterio-Huelin, D. Torricelli, and A. Gil-Agudo, "Quantitative assessment based on kinematic measures of functional impairments during upper extremity movements: A review," *Clin. Biomech.*, vol. 29, no. 7, pp. 719–727, 2014.
[27] J. Aizawa et al., "Three-dimensional motion of the upper extremity joints during various activities of daily living," *J. Biomech.*, vol. 43, no. 15, pp. 2915–2922, Nov. 2010.
[28] D. H. Gates, L. S. Walters, J. Cowley, J. M. Wilken, and L. Resnik, "Range of motion requirements for upper-limb activities of daily living," *Amer. J. Occupat. Therapy*, vol. 70, no. 1, pp. 7001350010-1–7001350010-10, Jan./Feb. 2016.
[29] C. P. Walmsley, S. A. Williams, T. Grisbrook, C. Elliott, C. Imms, and A. Campbell, "Measurement of upper limb range of motion using wearable sensors: A systematic review," *Sports Med. Open*, vol. 4, no. 1, pp. 1–22, Dec. 2018.
[30] E. E. Butler, A. L. Ladd, S. A. Louie, L. E. LaMont, W. Wong, and J. Rose, "Three-dimensional kinematics of the upper limb during a reach and grasp cycle for children," *Gait Posture*, vol. 32, no. 1, pp. 72–77, 2010.
[31] O. Heidari, J. O. Roylance, A. Perez-Gracia, and E. Kendall, "Quantification of upper-body synergies: A case comparison for stroke and non-stroke victims," in *Proc. Int. Design Eng. Tech. Conf. Comput. Inf. Eng. Conf.*, vol. 50152. New York, NY, USA: American Society of Mechanical Engineers, 2016, Art. no. V05AT07A032.
[32] L. Mailleux et al., "Clinical assessment and three-dimensional movement analysis: An integrated approach for upper limb evaluation in children with unilateral cerebral palsy," *PLoS ONE*, vol. 12, no. 7, Jul. 2017, Art. no. e0180196.
[33] A. Guzik-Kopyto et al., "Selection of kinematic and temporal input parameters to define a novel upper body index indicator for the evaluation of upper limb pathology," *Appl. Sci.*, vol. 12, no. 22, p. 11634, Nov. 2022.
[34] A. d'Avella and M. Tresch, "Modularity in the motor system: Decomposition of muscle patterns as combinations of time-varying synergies," in *Proc. Adv. Neural Inf. Process. Syst.*, vol. 14, 2001, pp. 1–8.
[35] A. d'Avella and F. Lacquaniti, "Control of reaching movements by muscle synergy combinations," *Frontiers Comput. Neurosci.*, vol. 7, p. 42, Apr. 2013.
[36] M. I. M. Refai et al., "Smoothness metrics for reaching performance after stroke. Part 1: Which one to choose?" *J. NeuroEng. Rehabil.*, vol. 18, no. 1, pp. 1–16, 2021.
[37] C. M. Kanzler et al., "A low-dimensional representation of arm movements and hand grip forces in post-stroke individuals," *Sci. Rep.*, vol. 12, no. 1, pp. 1–14, May 2022.
[38] M. G. Catalano, G. Grioli, E. Farnioli, A. Serio, C. Piazza, and A. Bicchi, "Adaptive synergies for the design and control of the pisa/IIT softhand," *Int. J. Robot. Res.*, vol. 33, no. 5, pp. 768–782, Apr. 2014.
[39] T. A. Lenssen, L. Cappello, D. H. Plettenburg, C. Cipriani, and M. Controzzi, "Principal orientations of the wrist during ADLs: Towards the design of a synergetic wrist prosthesis," in *Converging Clinical and Engineering Research on Neurorehabilitation III* (Biosystems & Biorobotics), vol. 21, L. Masia, S. Micera, M. Akay, and J. Pons, Eds. Cham, Switzerland: Springer, 2019. [Online]. Available: https://link.springer.com/chapter/10.1007/978-3-030-01845-0_68, doi: 10.1007/978-3-030-01845-0_68.
[40] G. Averta, C. D. Santina, E. Battaglia, F. Felici, M. Bianchi, and A. Bicchi, "Unvealing the principal modes of human upper limb movements through functional analysis," *Frontiers Robot. AI*, vol. 4, p. 37, Apr. 2017.
[41] G. Averta et al., "On the time-invariance properties of upper limb synergies," *IEEE Trans. Neural Syst. Rehabil. Eng.*, vol. 27, no. 7, pp. 1397–1406, Jul. 2019.
[42] Y. Gloumakov, A. J. Spiers, and A. M. Dollar, "Dimensionality reduction and motion clustering during activities of daily living: Three-, four-, and seven-degree-of-freedom arm movements," *IEEE Trans. Neural Syst. Rehabil. Eng.*, vol. 28, no. 12, pp. 2826–2836, Dec. 2020.
[43] J.-L. Wang, J.-M. Chiou, and H.-G. Müller, "Functional data analysis," *Annu. Rev. Stat. Appl.*, vol. 3, pp. 257–295, Jun. 2016.
[44] J. O. Ramsay and B. W. Silverman, *Functional Data Analysis*. New York, NY, USA: Springer-Verlag, 2005. [Online]. Available: https://link.springer.com/book/10.1007/b98888
[45] J. D. Tucker, W. Wu, and A. Srivastava, "Generative models for functional data using phase and amplitude separation," *Comput. Statist. Data Anal.*, vol. 61, pp. 50–66, May 2013.
[46] M. R. Cutkosky et al., "On grasp choice, grasp models, and the design of hands for manufacturing tasks," *IEEE Trans. Robot. Autom.*, vol. 5, no. 3, pp. 269–279, Jun. 1989.
[47] T. Feix, J. Romero, H.-B. Schmiedmayer, A. M. Dollar, and D. Kragic, "The GRASP taxonomy of human grasp types," *IEEE Trans. Human-Mach. Syst.*, vol. 46, no. 1, pp. 66–77, Feb. 2016.
[48] K. Abdel-Malek, J. Yang, R. Brand, and E. Tanbour, "Towards understanding the workspace of human limbs," *Ergonomics*, vol. 47, no. 13, pp. 1386–1405, 2004.
[49] J. C. Perry, J. Rosen, and S. Burns, "Upper-limb powered exoskeleton design," *IEEE/ASME Trans. Mechatronics*, vol. 12, no. 4, pp. 408–417, Aug. 2007.
[50] J. Ryu, W. P. Cooney, L. J. Askew, K.-N. An, and E. Y. S. Chao, "Functional ranges of motion of the wrist joint," *J. Hand Surg.*, vol. 16, no. 3, pp. 409–419, May 1991.
[51] D. L. Nelson, M. A. Mitchell, P. G. Groszewski, S. L. Pennick, and P. R. Manske, "Wrist range of motion in activities of daily living," in *Advances in the Biomechanics of the Hand and Wrist* (NATO ASI Series), vol. 256, F. Schuind, K. N. An, W. P. Cooney, and M. Garcia-Elias, Eds. Boston, MA, USA: Springer, 1994. [Online]. Available: https://link.springer.com/chapter/10.1007/978-1-4757-9107-5_29, doi: 10.1007/978-1-4757-9107-5_29.
[52] G. Wu et al., "ISB recommendation on definitions of joint coordinate systems of various joints for the reporting of human joint motion—Part II: Shoulder, elbow, wrist and hand," *J. Biomech.*, vol. 38, no. 5, pp. 981–992, May 2005.
[53] A. Murgia, P. J. Kyberd, P. H. Chappell, and C. M. Light, "Marker placement to describe the wrist movements during activities of daily living in cyclical tasks," *Clin. Biomech.*, vol. 19, no. 3, pp. 248–254, Mar. 2004.
[54] F. Yao, H.-G. Müller, and J.-L. Wang, "Functional data analysis for sparse longitudinal data," *J. Amer. Stat. Assoc.*, vol. 100, no. 470, pp. 577–590, 2005, doi: 10.1198/016214504000001745.
[55] F. Montagnani, M. Controzzi, and C. Cipriani, "Is it finger or wrist dexterity that is missing in current hand prostheses?" *IEEE Trans. Neural Syst. Rehabil. Eng.*, vol. 23, no. 4, pp. 600–609, Jul. 2015.
[56] N. M. Bajaj, A. J. Spiers, and A. M. Dollar, "State of the art in artificial wrists: A review of prosthetic and robotic wrist design," *IEEE Trans. Robot.*, vol. 35, no. 1, pp. 261–277, Feb. 2019.
[57] S. L. Carey, M. J. Highsmith, M. E. Maitland, and R. V. Dubey, "Compensatory movements of transradial prosthesis users during common tasks," *Clin. Biomech.*, vol. 23, no. 9, pp. 1128–1135, Nov. 2008.
[58] M. Yahya, J. A. Shah, K. A. Kadir, Z. M. Yusof, S. Khan, and A. Warsi, "Motion capture sensing techniques used in human upper limb motion: A review," *Sensor Rev.*, vol. 39, no. 4, pp. 504–511, Jan. 2019, doi: 10.1108/SR-10-2018-0270.
[59] K. Nizamis, N. Rijken, A. Mendes, M. Janssen, A. Bergsma, and B. Koopman, "A novel setup and protocol to measure the range of motion of the wrist and the hand," *Sensors*, vol. 18, no. 10, p. 3230, Sep. 2018.
[60] B.-S. Lin, I.-J. Lee, P.-Y. Chiang, S.-Y. Huang, and C.-W. Peng, "A modular data glove system for finger and hand motion capture based on inertial sensors," *J. Med. Biol. Eng.*, vol. 39, no. 4, pp. 532–540, Aug. 2019.

Open Access funding provided by 'Scuola Superiore "S.Anna" di Studi Universitari e di Perfezionamento' within the CRUI CARE Agreement